PSM Journals

PSM
Biological Research

Research Article 2024 | Volume 9 | Issue 1 | 1-8

Open Access

Article Information

Received: October 16, 2023

Accepted: October 26, 2023

Published: November 3, 2023

Keywords

Hypereutectic,
XRD,
Al-Si alloy,
Vickers hardness.

Authors' Contribution

OH and SA conceived and designed the study. All the authors were involved in writing and revising the paper.

† Both authors contributed equally to this manuscript.

How to cite

Humaid, O., Humaid, A.A., Alsowidy, S., Gumaan, M.S., 2024. Microstructure and Localized Plastic Deformation of Al/Si Alloy Improved with $CuAl_2$ Compound. PSM Biol. Res., 9(1): 1-8.

***Correspondence**

Olfat Humaid
Email:
o.humaid1234@gmail.com;
a.hamid@su.edu.ye

Microstructure and Localized Plastic Deformation of Al/Si Alloy Improved with $CuAl_2$ Compound

Olfat Humaid[†1,3], Abdulrahman A. Humaid[2*†], Shakib Alsowidy[3], Mohammed S. Gumaan[4]

[1]Physics Department, Faculty of Applied Science, Hajjah University, Yemen.
[2]Biology Department, Division of Microbiology, Faculty of Science, Sana'a University, Yemen.
[3]Laboratory of Materials Science, Physics Department, Faculty of Science, Sana'a University, Yemen.
[4]Biomedical Engineering Department, Faculty of Engineering, University of Science & Technology, Yemen.

Abstract:

The microstructure of Al-Si-xCu alloys with different percentages (x= 0, 0.1, 0.2, 0.3 wt. %) has been investigated using X-ray diffraction (XRD). Localized permanent plastic deformation (Vickers hardness (HV)) was conducted for all samples before and after the sintering process. From the XRD map, the Al-Si alloy consists of α-Al and Si phases while the Intermetallic compound (IMC) $CuAl_2$ has been detected with the addition of Cu. Also, it was found that there was a small shift in the peak position to the high angle as more Cu content was added. This shift is a result of the incoincidence of d_{hkl} levels in the Al-phase before and after the addition of Cu. This mismatch in d_{hkl} levels is associated with lattice defects and localized strain deformation. From Vickers hardness results, the formation of $CuAl_2$ precipitates promotes an increase in hardness from 11.643 Hv in the binary Al-Si to 27.439 Hv in the ternary Al-Si-0.3wt. % Cu whereas the highest value was found at 28.755 Hv with 0.2 wt. % of Cu after sintering. This is attributed to the temperature-promoting diffusion of copper atoms into Al lattices which improves hardness.

Scan QR code to visit this journal.

INTRODUCTION

Aluminium has a high strength-to-weight ratio, is ductile, and durable, and makes up 8% of the earth's surface weight as a mineral. These qualities have drawn the attention of modern researchers and enterprises to aluminium (Krishnan *et al.*, 2019; Raabe *et al.*, 2022). Due to the weak mechanical properties of pure aluminium, many works have been performed to enhance the properties of aluminium by alloying and heat treatment (Trivedi *et al.*, 2004). Al-Si alloy is being thoroughly studied due to its exceptional qualities, which include low coefficient of thermal expansion, superior wear and corrosion resistance, high strength-to-weight ratio, and good castability. Because of these characteristics, Al-Si alloys are used more frequently in the automobile sector, particularly for cylinder heads, cylinder blocks, pistons, and valve lifters (Kotadia *et al.*, 2010; Lasa and Rodriguez-Ibabe, 2003; Liao *et al.*, 2002; Taylor *et al.*, 2005; Warmuzek, 2004). Different elements are alloyed to Al-Si alloys to further enhance their properties (Callegari *et al.*, 2023). The current study is an attempt to improve the strength of the Al-Si alloy by adding traces of copper alloying elements.

MATERIAL AND METHODS

Materials Preparation

The nanopowder aluminium, silicon, and copper were accurately weighted in balance to make the required composition as shown in Table (1) with high purity of 99.99% for all elements. The balanced elements were mixed in a powder form at room temperature and then subjected to compression using a hydraulic pressure system with a constant load of 250KN for 5 minutes for all samples. The compacted cylindrical disks were obtained with dimensions of 6 × 32 mm. After that, the compressed samples were sintered in a controlled atmosphere furnace at about 450 °C to allow the bounding of particles for each other. For X-ray diffraction (XRD) analysis, a ShimadzuX–ray diffractometer (EDX-720) with Cu kα radiation (λ = 1.54056 A^{o}) was used to determine the alloy phases, and then identify other lattice parameters. Vickers hardness test (localized plastic deformation resistance or impact force resistance) has been performed using the mechanical equipment as shown in Figure (1) (Polanco *et al.*, 2022).

Table 1. Chemical composition of Al-Si-xCu alloys.

Chemical compositions (Wt.%)				
Alloys	**Samples**	**Al**	**Si**	**Cu**
Al-Si	A1	Balance	17	0
Al-Si-0.1Cu	A2	Balance	17	0.1
Al-Si-0.2Cu	A3	Balance	17	0.2
Al-Si-0.3Cu	A4	Balance	17	0.3

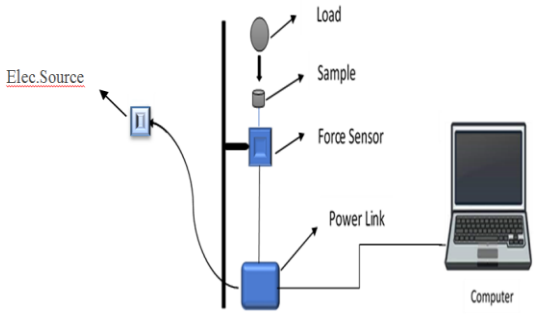

Fig.1. Schematic diagram of Vickers hardness tester.

RESULTS AND DISCUSSION

XRD Analysis

X-ray diffraction is a popular characterization technique that is used to determine phases present in metal alloys. The diffraction pattern obtained is shown in Figures (2a),(2b),(2c) and (2d). It can be seen that the Al-Si alloy is primarily composed of two phases identified as the α-Al phase and Si phase. The lines (111, 200, and 220) represent the Al-phase, and the lines (111, 220, 311, and 400) represent the Si phase. This result is in good agreement with the previous literature (Santos *et al.*, 2021). A new phase is deduced with the addition of Cu as shown in Figures (2b),(2c), and (2d). According to the Al-Cu phase diagram (Massalski *et al.*, 1986), and from the previous literature (An *et al.*, 2022), this intermetallic compound (IMC) is $CuAl_2$. When comparing Al peaks before and

after Cu addition, there is a small shift in the peak position to the high angle as more Cu content is added as shown in Table (2) and Figure (3). This shift in the angle position reflects itself in the incoincidence of interplanar spacing (d_{hkl}) levels before and after Cu-addition as confirmed by the values in Table (3). This incoincidence of (d_{hkl}) levels is associated with the lattice defects, localized strain deformation, and change in lattice parameters of Al lattice as confirmed by the values in Table (4). This may be attributed to the Cu atom dissolution and diffusion on the Al lattice.

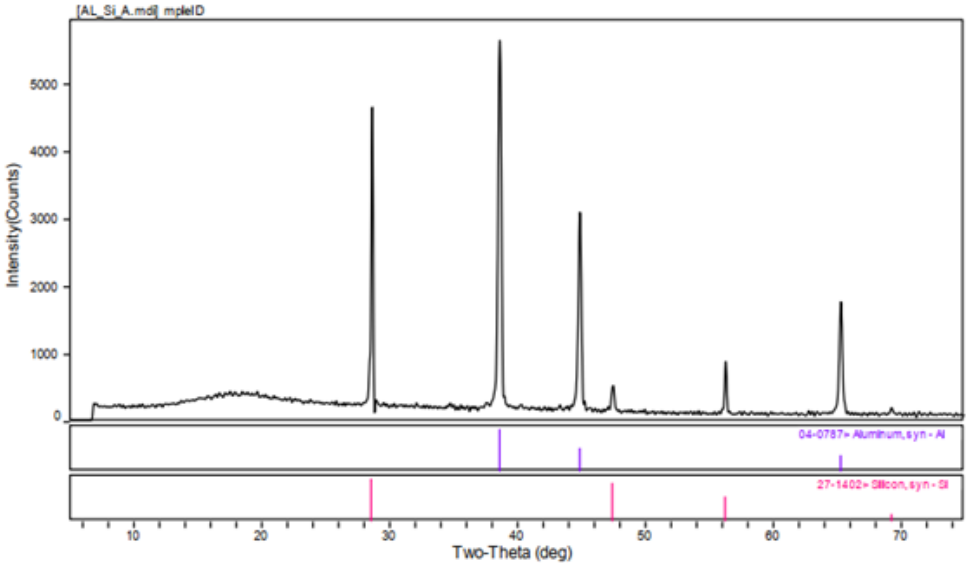

Fig. 2a. XRD pattern of A1 alloy.

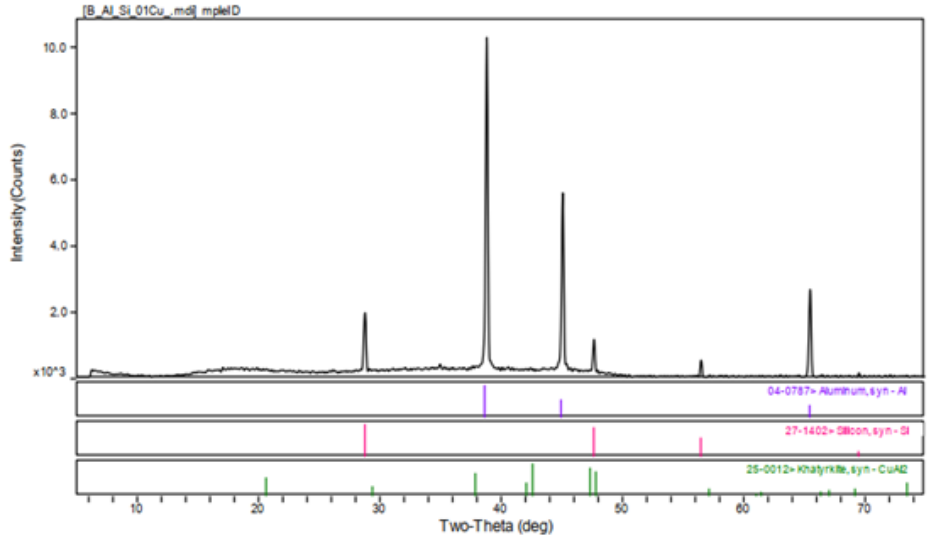

Fig. 2b. XRD pattern of A2 alloy.

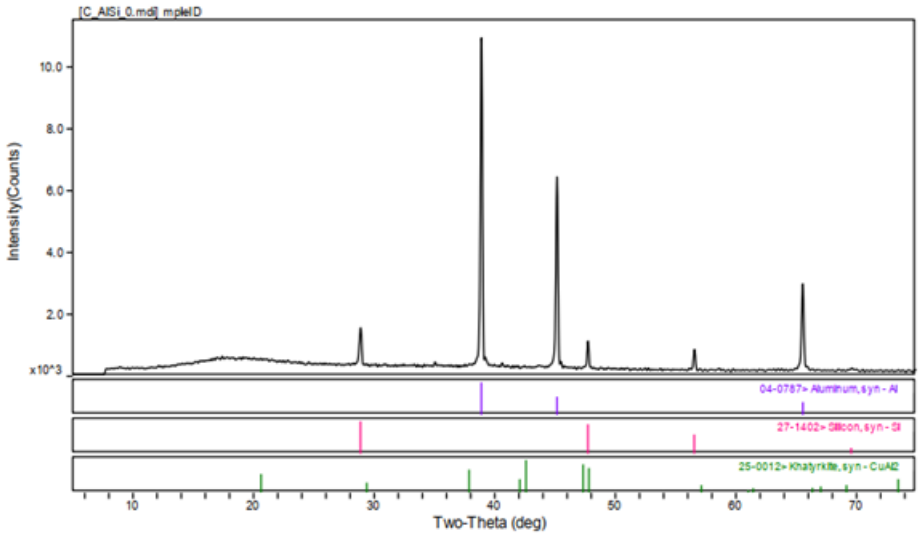

Fig. 2c. XRD pattern of A3 alloy.

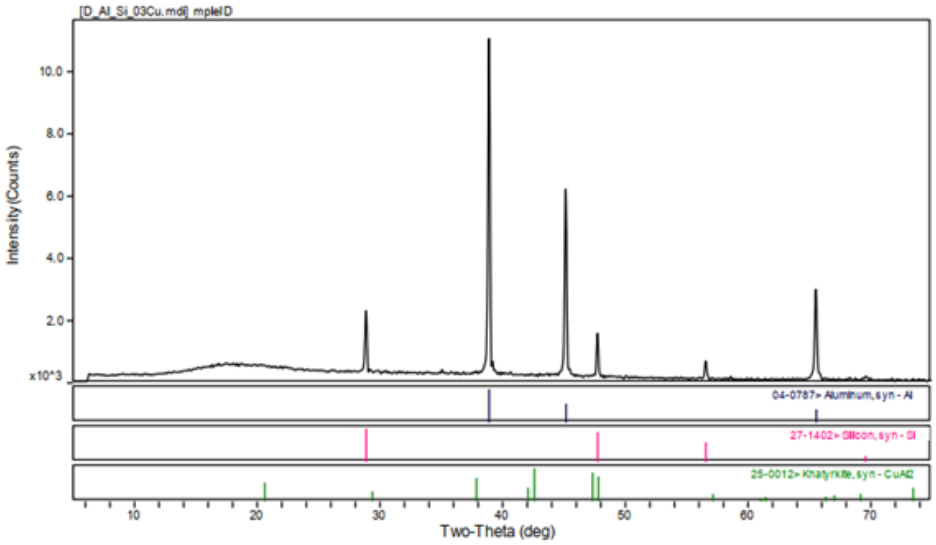

Fig. 2d. XRD pattern of the A4 alloy.

Table 2. The angle position of Al lines for all samples.

Lines	**2ɵ(deg)**			
	A1	**A2**	**A3**	**A4**
111	38.6	38.82	38.9	38.899
200	44.879	45.08	45.16	45.14
220	65.28	65.461	65.54	65.521

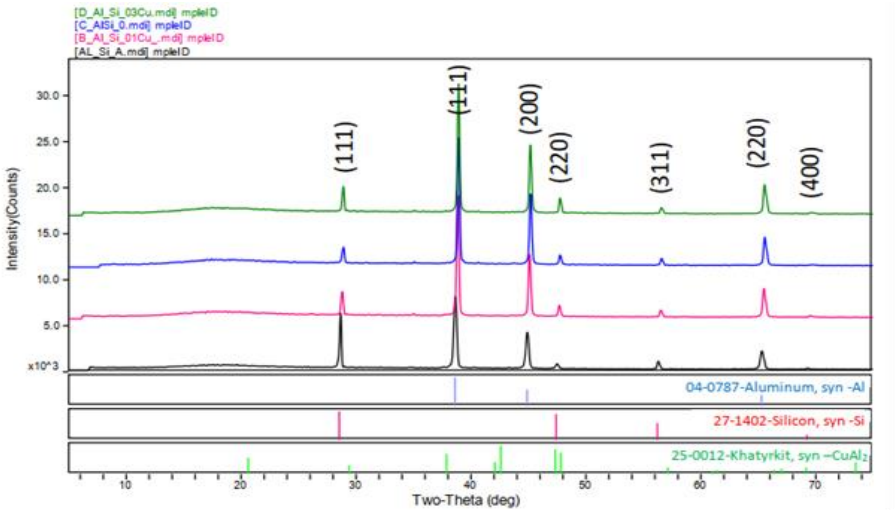

Fig. 3. The XRD patterns of Al-Si-xCu alloys.

Table 3. The interplanar spacing of Al lines for all samples.

Lines	$d_{hkl}(A^o)$			
	A1	**A2**	**A3**	**A4**
111	2.3305	2.3178	2.3132	2.3133
200	2.018	2.0095	2.0061	2.0069
220	1.4281	1.4246	1.4231	1.4235

Table 4. The lattice parameter of Al lines for all samples.

Lines	Lattice constant (A^o), a=b=c			
	A1	**A2**	**A3**	**A4**
111	4.0365	4.0145	4.0066	4.0068
200	4.036	4.019	4.0122	4.0138
220	4.0393	4.0294	4.0251	4.0263

According to the Scherrer formula (Patterson, 1939), the particle size is calculated and tabulated in Table (5).

$$D = 0.9\ \lambda/\beta\ \text{Cos}\theta \qquad (1)$$

where D is the crystallite size, θ is the Bragg angle, λ is the X-ray wavelength, and β is the broadening of the diffraction line measured at half its maximum intensity (radians). It can be seen from Table (5), that the particle size after Cu addition has more size than before. This is further evidence for the occurrence of Cu atoms diffusion into Al lattices.

The length of dislocation lines per unit volume of the crystal is known as the dislocation density (δ), which indicates the quantity of flaws in the sample. This dislocation density is calculated using the following equation:

$$\delta = 1 / D^2 \qquad (2)$$

where (D) is the average crystallite size (Dhanam *et al.*, 2008). The inverse relation between δ and D is shown in Figure (4) and Table (5).

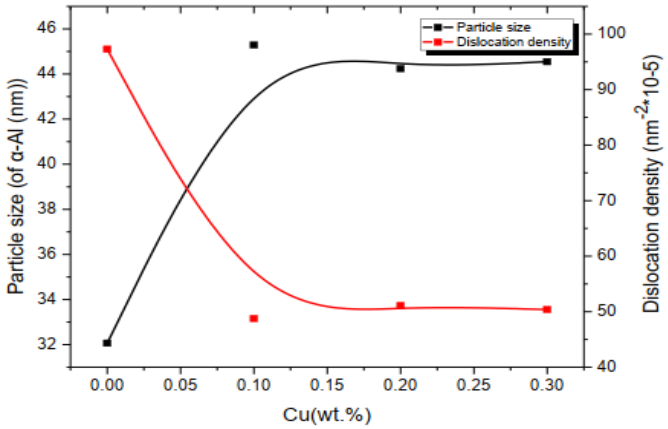

Fig. 4. Particle size and dislocation density as a function of Cu addition.

Table 5. Particle size and dislocation density of Al-Si-xCu alloys.

Alloys	Particle size (nm) of α-Al Phase (D)	Dislocation density(nm^{-2}) (δ) *10^{-5}
A1	32.061	97.285
A2	45.285	48.763
A3	44.24	51.094
A4	44.549	50.388

Vickers Hardness Measurements

The hardness property of the material is a very important mechanical property particularly, in structural applications. Vickers hardness was determined before and after the sintering process using the following formula (Krishna and Karthik, 2015),

$$Hv = 1.85\ L / d^2 \qquad (3)$$

Where L is the indentation load in kg and d is the mean diagonal of the indentation in mm.

Table (6) and Figure (5) show the Vickers hardness results obtained. It is clear that: (i) the higher copper content in the alloy means the higher the hardness value. This agrees with the finding of a previous study (Zeren and Karakulak, 2009) and (ii) the Vickers hardness after the sintering process is higher than that before sintering. This increment was explained by a previous research (Ciołek *et al.*, 2019). The maximum number of finely distributed particles in the aluminium matrix can be produced by sintered samples, according to their findings, which results in the most noticeable improvement in hardness.

Table 6. Vickers Hardness Number of Al-Si-xCu.

Alloys	**Vickers Hardness (Hv)**	
	Before Sintering	**After Sintering**
A1	11.643	13.1317
A2	12.735	13.657
A3	14.7696	28.755
A4	27.439	18.153

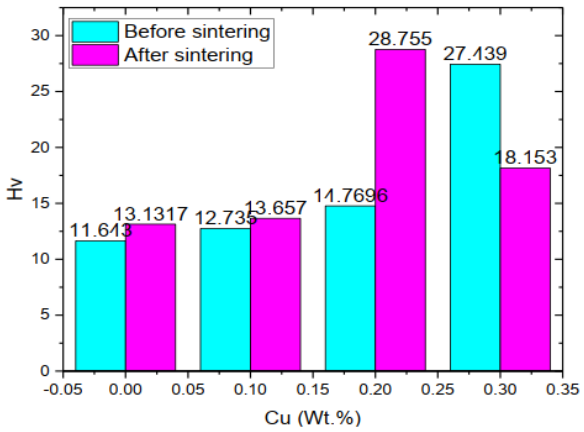

Fig. 5. Vickers hardness as a function of Cu content.

CONCLUSION

The effect of Cu on the microstructure and mechanical properties (hardness) of Al-Si-xCu alloys were investigated. The results are summarized as follows:

1- From X-ray diffraction (XRD), the microstructure of Al-Si alloy consists of two phases identified as α-Al phase and Si phase.

2- The presence of alloying elements such as Cu leads to the formation of intermetallic compounds; the presence $CuAl_2$ phase in the microstructure strengthens the Al-Si alloy.

3- The formation of $CuAl_2$ precipitates promotes an increase in hardness from 11.643 Hv in the binary Al-Si to 27.439 Hv in the ternary Al-Si-0.3wt.% Cu. This phase impeded the movement of dislocations, and as a result, the alloy has high hardness.

4- The highest value was 28.755 Hv with 0.2wt. % of Cu after sintering. This is attributed to the temperature promoting diffusion of copper atoms into Al lattices which improves hardness.

ACKNOWLEDGMENT

The authors would like to express their thankfulness to the Physics Department, Faculty of Science, Sana'a University-Yemen for their assistance and facilitating this work. Also, the authors would like to express their thanks to the Laboratory of Materials Science, Physics Department, Faculty of Science, Sana'a University-Yemen, and Yemen Geological Survey and Mineral Resources Board (YGSMRB)-Sana'a for carrying out this work.

CONFLICT OF INTEREST

Authors hereby declare that they have no conflict of interest.

REFERENCES

An, S., Kim, M., Huh, C., Kim, C., 2022. Microstructure and Mechanical Property of Al6Si2Cu Alloy Subjected to Double-Solution Heat Treatment. Metals., 12(1): 18.

Callegari, B., Lima, T.N., Coelho, R.S., 2023. The Influence of Alloying Elements on the Microstructure and Properties of Al-Si-Based Casting Alloys: A Review. Metals, 13(7): 1174.

Ciołek, S., Jóźwiak, S., Karczewski, K., 2019. Possibility of Strengthening Aluminum Using Low-Symmetry Phases of the Fe-

Al Binary System. Metall. Mater. Trans. A., 50(4): 1914-1921.

Dhanam, M., Prabhu, R.R., Manoj, P., 2008. Investigations on chemical bath deposited cadmium selenide thin films. Mater. Chem. Phys., 107: 289-296.

Kotadia, H.R., Hari Babu, N., Zhang, H., Fan, Z., 2010. Microstructural refinement of Al–10.2%Si alloy by intensive shearing. Mater. Lett., 64(6): 671-673.

Krishna, S., Karthik, M., 2015. Evaluation of Hardness Strength of Aluminium Alloy (AA 6061) Reinforced With Silicon Carbide.

Krishnan, P. et al., 2019. Production of aluminum alloy-based metal matrix composites using scrap aluminum alloy and waste materials: Influence on microstructure and mechanical properties. J. Alloys Compd., 784.

Lasa, L., Rodriguez-Ibabe, J.M., 2003. Wear behaviour of eutectic and hypereutectic Al–Si–Cu–Mg casting alloys tested against a composite brake pad. Mater. Sci. Eng: A., 363(1): 193-202.

Liao, H., Sun, Y., Sun, G., 2002. Correlation between mechanical properties and amount of dendritic α-Al phase in as-cast near-eutectic Al–11.6% Si alloys modified with strontium. Mater. Sci. Eng: A., 335: 62-66.

Massalski, T.B., Murray, J.L., Bennett, L.H., Baker, H., 1986. Binary alloy phase diagrams. American Society for Metals Metals Park, Ohio, Metals Park, Ohio.

Patterson, A.L., 1939. The Scherrer Formula for X-Ray Particle Size Determination. Phys. Rev., 56(10): 978-982.

Polanco, J.D., Jacanamejoy-Jamioy, C., Mambuscay, C.L., Piamba, J.F., Forero, M.G., 2022. Automatic Method for Vickers Hardness Estimation by Image Processing. J. Imag., 9(1).

Raabe, D. et al., 2022. Making sustainable aluminum by recycling scrap: The science of “dirty” alloys. Prog. Mater. Sci., 128: 100947.

Santos, S., Toloczko, F., Merij, A., Saito, N., Silva, D., 2021. Investigation and Nanomechanical Behavior of the Microconstituents of Al-Si-Cu alloy After Solution and Ageing Heat Treatments. Mater. Res., 24.

Taylor, J., Couper, M., Smith, C.L., Singh, D.P.K., 2005. Dissolution, recovery and fade of SR master alloys in AL-7SI-0.5MG casting alloy. TMS Light Metals.

Trivedi, P., Field, D., Weiland, H., 2004. Alloying effects on dislocation substructure evolution of aluminum alloys. Int. J. Plastic., 20.

Warmuzek, M., 2004. Aluminum-silicon casting alloys : an atlas of microfractographs. ASM International Materials Park, OH, Materials Park, OH.

Zeren, M., Karakulak, E., 2009. Study on hardness and microstructural characteristics of sand cast Al–Si–Cu alloys. Bull. Mater. Sci., 32: 617-620.